

HiSIM: A Drift-Diffusion-Based Advanced MOSFET Model for Circuit Simulation with Easy Parameter Extraction

M. Suetake, K. Suematsu, H. Nagakura, M. Miura-Mattausch, H. J. Mattausch*

Department of Electrical Engineering, *Research Center for Nanodevice and Systems, Hiroshima University
1-4-1, Kagamiyama, Higashi-Hiroshima, 739-8527, Japan

S. Kumashiro, T. Yamaguchi, S. Odanaka^a, and N. Nakayama

Semiconductor Technology Academic Research Center
Onarimon BN Bldg., 16-10, Shimbashi 6-chome, Minato-ku, Tokyo, 105-0004, Japan

Abstract— We present here the MOSFET-model HiSIM. Since HiSIM employs the drift-diffusion approximation and preserves a correct modeling of the surface potential in the channel, it is not only accurate. Additionally model-parameter number is small, parameter interdependence is removed, and parameter extraction becomes easy. Measured current-voltage characteristics of advanced MOSFETs is thus reproduced with only 19 model parameters.

I. INTRODUCTION

ADVANCED MOSFET performance is determined by new phenomena e.g. quantum effects, poly-depletion effects or gate leakage currents. Of course, these phenomena must be correctly implemented in MOSFET models for circuit simulation. However, extraction of model parameters for conventional MOSFET models is already extremely complicated. Moreover, extracted parameter values have often lost their original physical meaning, especially due to the conventional modeling-approach of short-channel (SC) effects. Therefore, a revision of the model basics is an urgent necessity, to keep future circuit simulation practical.

We describe here the MOSFET-model HiSIM (Hiroshima-university Starc IGFET Model) with a focus on its parameter extraction. HiSIM employs the drift-diffusion approximation and preserves a correct modeling of the surface potential (ϕ_S) in the channel. It is therefore not only accurate, but additionally model-parameter number is small, parameter interdependence is largely removed, and parameter extraction becomes easy. In comparison to conventional MOSFET models parameters number is reduced to about 1/5 at a comparable level of accuracy.

II. MODELING OF PHYSICAL PHENOMENA

HiSIM determines ϕ_S iteratively and models the SC effects by the derivative of the lateral electric field in the ϕ_S equations. In spite of the iteration the total simulation time is less than for conventional models [1]. The reverse-short-channel (RSC) effects are modeled with channel-length-dependent doping profiles, which are extracted from the measured threshold-bulk voltage ($V_{th} - V_{bs}$) characteristics [2]. Besides these technology-related quantities, further

^a Present address: Cybermedia Center, Osaka University, 1-1, Machikaneyama, Toyonaka, Osaka, 560-0043, Japan.

physical phenomena, already known to be unavoidable for advanced technologies, are modeled as follows.

A. Quantum Effects (QE)

The necessity for including quantum effects (QE) has been obvious since the reduction of the gate-oxide thickness T_{ox} approaches its limit. The main effect is that the peak of the carrier density distribution is pushed away from the surface into the channel. This can be described phenomenologically by a T_{ox} increase. Two major approximations are introduced for a simple description: First, a triangular potential perpendicular to the channel is assumed. Second, carriers are restricted to occupy only the lowest energy level. Resulting effective oxide thickness T_{oxeff} becomes [3,4]

$$\begin{aligned} T_{oxeff} &= T_{ox} + \alpha(Q_b + \frac{11}{32}Q_{inv})^{-\frac{1}{3}} \\ \alpha &= \frac{48\pi m_e}{\epsilon_{Si} \hbar^2 q} = 3.5 \times 10^{-10} (Ccm)^{\frac{1}{3}} \end{aligned} \quad (1)$$

where Q_b and Q_{inv} are bulk- and inversion charge density, respectively. Other parameters have the same meaning as in [3]. The coefficient α , originally derived quantum mechanically under above mentioned approximations, is treated as a fitting parameter.

B. Gate-Poly Depletion Effects (PDE)

The gate-poly depletion effects (PDE) are modeled with a low-impurity-concentration region (N_{pg}) in the gate-poly Si. For this purpose the Poisson equation and (2) are solved simultaneously in the substrate and the gate-poly Si (poly-Si) with an iteration procedure.

$$V_{gs} - V_{fb} - \phi_S - \phi_{pg} = \frac{\epsilon_S E_S}{C_{ox}} \quad (2)$$

Here V_{gs} , V_{fb} , ϕ_S , ϕ_{pg} , E_S , are gate voltage, flat-band voltage, surface potential in the Si substrate, surface potential in the poly-Si, and vertical electric field in the substrate, respectively. Fig. 1 shows calculation result of ϕ_S and ϕ_{pg} as a function of poly-Si impurity concentration. The depletion in the poly-Si occurs after the starting of the strong inversion in the bulk Si, where the impurity concentration is

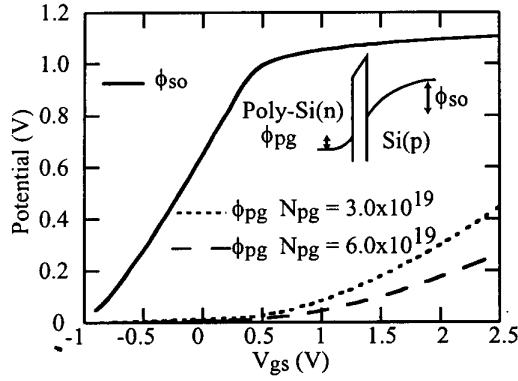


Fig. 1. Surface potential in substrate (solid curve) and in poly-Si (dashed curves) as a function of gate voltage V_{gs} at source side.

much lower than in the poly-Si. Fig. 2 compares measured transconductance g_m as a function of V_{gs} with 2D simulation results, excluding and including the depletion in the poly-Si, respectively. This comparison demonstrates the influence of poly-Si depletion effects on MOSFET performance, which becomes substantial after the onset of strong inversion, and therefore confirms the result given in Fig. 1. For optimized calculation time the Poisson equation in the poly-Si region can be simplified by ignoring inversion carriers. Thus the iteration, otherwise necessary to obtain consistent ϕ_{pg} values, can be eliminated.

C. Carrier Mobility

The carrier mobility is described by the following expression with 3 independent contributions [5]:

$$\frac{1}{\mu_0} = \frac{1}{\mu_C} + \frac{1}{\mu_{Ph}} + \frac{1}{\mu_{SR}} \quad (3)$$

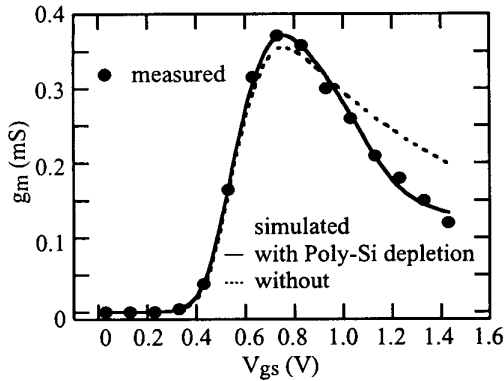


Fig. 2. Measured and simulated transconductance g_m vs. gate-source (V_{gs}) voltage.

$$\mu_C(\text{Coulomb}) = X1 + X2 \frac{N_{inv}}{10^{11}} \quad (4)$$

$$\mu_{Ph}(\text{phonon}) = \frac{Y1}{T \times E_{eff}^{Y2}} \quad (5)$$

$$\mu_{SR}(\text{surface roughness}) = \frac{Z1}{E_{eff}^{Z2}} \quad (6)$$

$$E_{eff} = \frac{1}{\epsilon_{Si}} (Q_b + \frac{1}{2} Q_{inv}) \quad (7)$$

Here N_{inv} is the carrier concentration at threshold ($1 \times 10^{11} \text{ cm}^{-2}$). T is the lattice temperature, and E_{eff} is the effective field normal to the surface. $X1$, $X2$, $Y1$, $Z1$ are fitting parameters. Due to the universality of μ_0 at low fields along the channel direction, $Y2=0.3$ and $Z2 \simeq 1$ are known to be practically independent of technology variations. The high-field mobility is modeled as

$$\mu = \frac{\mu_0}{(1 + (\frac{\mu_0 E_y}{V_{sat}})^\beta)^{\frac{1}{\beta}}} \quad (8)$$

where $\beta = 2$ for electrons. $V_{sat} \simeq 1 \times 10^7 \text{ cm/s}$ is the electron saturation velocity, and E_y is the electric field along the channel. E_y is determined by the ϕ_S gradient. It has been recognized that β should be an even integer value to secure the continuity at $V_{ds} = 0$ [6].

III. PARAMETER EXTRACTION PROCEDURE

Parameter extraction for HiSIM needs the following steps (see Fig. 3):

A. Extraction of Channel Impurity Profile

The channel impurity profile ($N_{sub}(x)$) is extracted from measured $V_{th} - V_{bs}$ characteristics for each gate length L_{gate} [2]. For simplicity $N_{sub}(x)$ is modeled as a linear function of depth x

$$N_{sub}(L_{gate}, x) = N_{sub0}(L_{gate}) + N_{subg}(L_{gate}) \times x \quad (9)$$

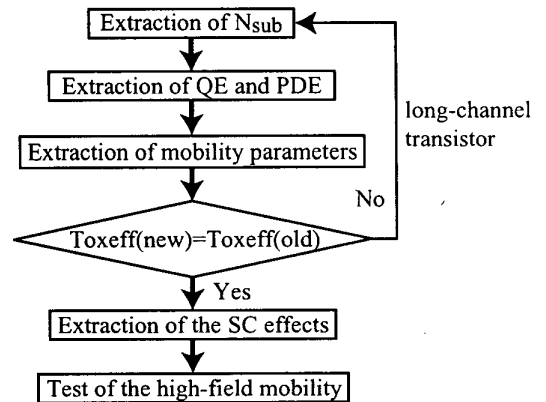


Fig. 3. Parameter extraction procedure.

where $N_{sub0}(L_{gate})$ and $N_{subg}(L_{gate})$ are the parameters to be extracted. First, physical T_{ox} is used and PDE are ignored. With this data Q_b and Q_{inv} can be calculated by solving ϕ_S iteratively with $T_{oxeff} = T_{ox}$.

B. Extraction of QE

Parameter extraction of QE means to determine just the single parameter α . For this purpose the measured C-V characteristics at relative small V_{gs} values are fitted as shown in Fig. 4. Since the PDE are superposed above threshold condition, this region of the C-V characteristics is not used for the determination of α .

C. Extraction of PDE

Extraction of PDE is also done with just 1 parameter, namely the poly-Si doping N_{pg} . Again the measured C-V characteristics is fitted, however, in this case above V_{th} as shown in Fig. 4.

QE and PDE parameters are extracted iteratively by repeating the steps from (1) to (4) until the newly calculated T_{oxeff} becomes equal to the previous one. This iteration is required to obtain self-consistent model parameter values. Fortunately, just 1 iteration is needed under normal circumstances. Up to step (4) only a long-channel transistor is employed.

D. Extraction of Parameters for Short-Channel (SC) and Reverse-Short-Channel (RSC) Effects

Extraction of the 3 parameters invested for modeling the SC effects and the 9 parameters for modeling the RSC effects is performed with measured $V_{th} - V_{bs}$ characteristics for short-channel transistors [2]. The 9 RSC parameters are needed to describe the L_{gate} dependence of the vertical impurity profile by a simple equation. For normal application 3 of them can be ignored.

Though N_{sub} is modified by inclusion of the RSC effects, influence on T_{oxeff} turns out to be almost negligible. Fig. 5 shows a comparison of the real oxide thickness T_{ox} and

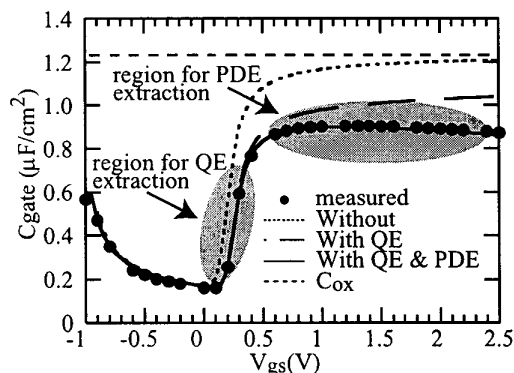


Fig. 4. Comparison of measured C-V characteristics with simulation results for different models.

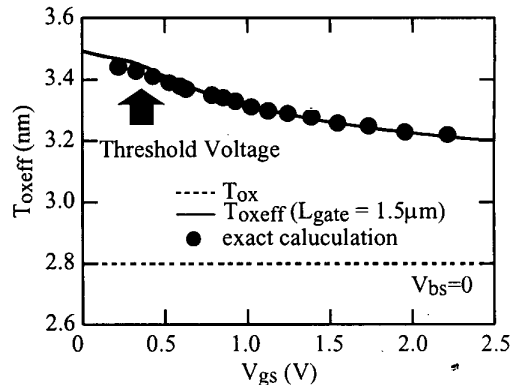


Fig. 5. Calculated T_{oxeff} including quantum effects (QE) and gate-poly depletion effects (PDE).

T_{oxeff} for the case of a long ($1.5\mu m$) channel. The T_{oxeff} dependence on V_{gs} , as calculated with HiSIM, and the exact calculation, solving the Schrödinger equation and the Poisson iteratively [7], are found to be in very good agreement. Fig. 6 shows calculated V_{th} as a function of L_{gate} for different V_{bs} values together with measurements [8].

E. Extraction of Parameters for the Mobility

Mobility parameters are extracted from measured I-V characteristics. Due to the small number of fitting parameters, extraction turns out to be quite easy in practice. Finally the high-field-mobility coefficient $\beta = 2$ is proved.

IV. CALCULATED RESULTS

Extracted parameters are shown in Table 1. Resulting I-V characteristics for short and long-channel transistors are compared with measured results [8] in Figs. 7 and 8.

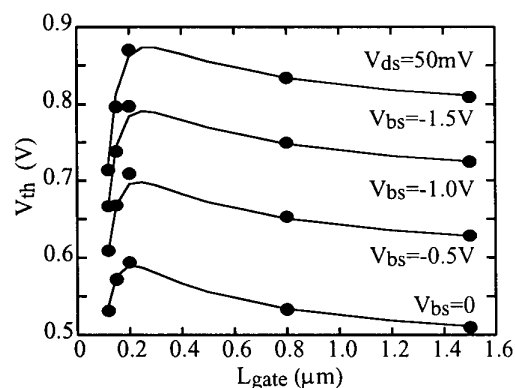


Fig. 6. Calculated threshold voltage including QE. Symbols are measurements and lines are calculated. Both the reverse-short-channel (RSC) effect and the short-channel (SC) effect are correctly expressed.

TABLE I
THE PARAMETER LIST.

| parameter | value | dimension |
|---------------|-------------------------|--|
| <i>QDEPCC</i> | -2.642×10^{-8} | RSC parameter |
| <i>QDEPCL</i> | 3.309×10^{-13} | RSC parameter |
| <i>QDEPCS</i> | 0.5 | RSC parameter |
| <i>QDEPBC</i> | 3.648×10^{-7} | RSC parameter |
| <i>QDEPBL</i> | 7.705×10^{-13} | RSC parameter |
| <i>QDEPBS</i> | 1 | RSC parameter |
| <i>VFBC</i> | -0.708 | RSC parameter |
| <i>VFBL</i> | 1.35×10^{-6} | RSC parameter |
| <i>VFBS</i> | 0.5 | RSC parameter |
| <i>SC1</i> | 14 | SC parameter |
| <i>SC2</i> | 2.7 | SC parameter |
| <i>PARL2</i> | 1×10^{-6} | SC parameter |
| <i>X1</i> | 300 | $cm^2/(V \times s)$ |
| <i>X2</i> | 30 | $cm^2/(V \times s)$ |
| <i>Y1</i> | 6.5×10^6 | $cm^{1.7} \times K/(V^{0.7} \times s)$ |
| <i>Y2</i> | 0.3 | no fitting |
| <i>Z1</i> | 10^{12} | cm/s |
| <i>Z2</i> | 1.4 | no dimension |
| α | 5×10^{-10} | $(C \times cm)^{\frac{1}{3}}$ |
| N_{poly} | 7.5×10^{19} | cm^{-3} |
| β | 2 | no fitting |

This comparison verifies the unique capability of HiSIM to correctly simulate advanced MOSFET characteristics from long gate length ($1.5\mu m$) to extremely short gate length ($0.12\mu m$) and from the subthreshold region up to the saturation region with a single set of only 19 parameters.

V. CONCLUSIONS

In this paper we have presented the advanced MOSFET model for circuit simulation HiSIM (*H*iros*H*shima-university *S*tarc *I*GFET *M*odel) and focused on HiSIMs simple and easy-to handle parameter extraction methodology. The main reason for the simplicity is that HiSIM requires only 19 model parameters for a complete modeling of advanced MOSFETs, including short-channel (SC), reverse-short-channel (RSC), quantum (QE) and gate-poly depletion (PDE) effects. Parameter interdependence is largely removed due to the physics-based modeling of above mentioned effects. This has to be compared to the nearly 100 largely interdependent parameters, needed by conventional MOSFET models for reaching a comparable level of accuracy.

REFERENCES

[1] M. Miura-Mattausch, U. Feldmann, A. Rahm, M. Bollu, and D. Savignac, "Unified complete MOSFET model for analysis of digital and analog circuits," *IEEE Trans. CAD/ICAS*, vol. 15, pp.1-7, Jan. 1996.

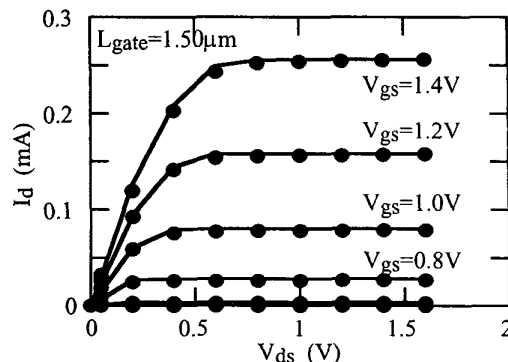


Fig. 7. $I_d - V_{ds}$ results for a long channel transistor in advanced technology.

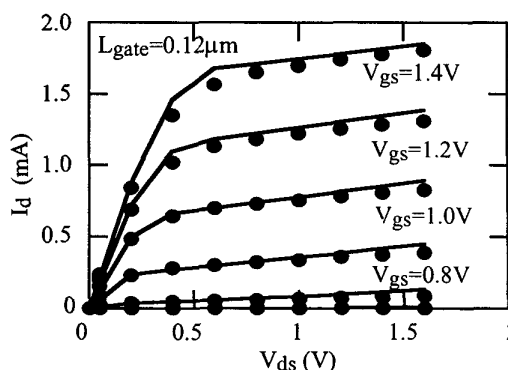


Fig. 8. $I_d - V_{ds}$ results for a short channel transistor in advanced technology.

[2] M. Suetake, M. Miura-Mattausch, H. J. Mattausch, S. Kumashiro, N. Shigyo, S. Odanaka, and N. Nakayama, "Precise physical modeling of the reverse-short-channel effect for circuit simulation", in *Proc. Intern. Conf. on Simulation of Semiconductor Processes and Devices (SISPAD'99)*, pp.207-210, 1999.

[3] F. Stern and W. E. Howard, "Properties of semiconductor surface inversion layers in the electric quantum limit", *Phys. Rev.*, vol. 163, Nov. 1967.

[4] Z. Yu, R. W. Dutton, and R. A. Kiehl, "Circuit device modeling at the quantum level", in *Proc. IWCE-6*, pp.222-229, 1998.

[5] S. Takagi, M. Iwase, and A. Toriumi, "On the universality of inversion-layer mobility in n- and p-channel MOSFETs", in *IEDM Tech. Dig.*, pp. 398-401, 1988.

[6] K. Joardar, K. K. Gullapalli, C. C. McAndrew, M. E. Burnham, and A. Wild, "An improved MOSFET model for circuit simulation", *IEEE Trans. Electron Dev.*, vol. 45, pp.134-148, Jan. 1998.

[7] T. Takahashi, M. Miura-Mattausch, and Y. Omura, "Transconductance oscillations in metal-oxide-semiconductor field-effect transistors with thin silicon-on insulator originated by quantized energy levels", *Appl. Phys. Lett.*, vol. 75, Sept. 1999.

[8] K. Takeuchi, T. Yamamoto, A. Furukawa, T. Tamura, and K. Yoshida, "High performance sub-tenth micron CMOS using advanced boron doping and WSi/sub 2/ dual gate process", in *Proc. Symposium on VLSI Technology*, pp. 9-10, 1995.